FRONT MATTER

Title

- Return of the Ritonavir: A Study on the Stability of Pharmaceuticals Processed in Orbit and Returned to Earth

Authors

Haley C. Bauser[1], Pamela A. Smith[2], Stephan. D. Parent[2], Larry R. Chan[1], Ami S. Bhavsar[1], Kenneth H. Condon[1], Andrew McCalip[1], Jordan M. Croom[1], Dale K. Purcell[2], Susan J. Bogdanowich-Knipp[2], Daniel T. Smith[2], Brett A. Cowans[2], Ruba Alajlouni[2], Stephen R. Byrn[2], and Adrian Radocea*[1]

Affiliations

1. Varda Space Industries, El Segundo, California 90245, United States
2. Improved Pharma LLC, West Lafayette, Indiana 47906, United States

*Corresponding author. Email: adrian@varda.com

Abstract

Despite notable progress in realizing the benefits of microgravity, the physical stability of therapeutics processed in space has not been sufficiently investigated. Environmental factors including vibration, acceleration, radiation, and temperature, if not addressed could impact the feasibility of in-space drug processing. The presented work demonstrates the successful recovery of the metastable Form III of ritonavir generated in orbit. The test samples and passive controls containing each of the anhydrous forms of ritonavir; Form I, Form II, Form III, and amorphous exhibit excellent stability. By providing a detailed experimental dataset centered on survivability, we pave the way for the future of in-space processing of medicines that enable the development of novel drug products on Earth and benefit long-duration human exploration initiatives.

Teaser

The metastable Form III of ritonavir was successfully crystallized in orbit and subsequentially recovered after reentry to Earth.

MAIN TEXT

Introduction

Early proof-of-concept demonstrations conducted on parabolic flights and on extended microgravity platforms such as the international space station (ISS) have demonstrated the potential benefits of in-space microgravity crystallization for better understanding polymorphism and for supporting pathfinding routes towards novel formulations (*1-4*). Polymorphic control of active pharmaceutical ingredients is a key concern for safety, manufacturability, and dosing (*5*,*6*). Unexpected interconversion from one form to a previously undiscovered, more stable form is often an unwanted scenario, most famously exhibited in the recall of ritonavir (*6*). As a result, understanding stability

and form conversion risks in space environments is a key concern for future space-based medicines and microgravity development (*7*).

Stability testing of pharmaceuticals stored on the International Space Station has highlighted that over a period of two years, a shift in potency was observed – though well within the expected shelf-life of the pharmaceuticals (*7,8*). Prior studies were limited in scope and focused primarily on chemical degradation during extended storage in orbit. The work raised additional questions to be addressed with solid state characterization of drug materials through standard means employed for pharmaceuticals, namely DSC, Raman and XRPD to understand the solid form evolution. Furthermore, questions on the influence of launch and reentry on the state of drug materials were not sufficiently addressed. Previous studies have been hampered, at least partially, by the limited and infrequent retrieval of materials from orbit and so extensive post-flight characterization to assess both the polymorphic state and chemical stability of pharmaceuticals processed has not yet been shown (*9-11*). The presented work is the first of its kind to analyze the stability of a pure pharmaceutical ingredient (API) processed in space as prior stability studies focus on marketed pharmaceuticals with their respective excipients and shelf stability mechanisms fully incorporated. By analyzing the stability of the pure API, we can examine the feasibility of in-orbit pharmaceutical development.

The HIV protease inhibitor ritonavir was selected for its particularly challenging polymorphic landscape which enables assessment of form interconversion for small molecules crystallized in space (*6,12,13*). An additional factor for its selection is its suitability for melt/cool crystallization (*12,13*). The crystallization process was tuned for the production of the metastable Form III from the melt of stable Form II. Form III is the crystalline form most vulnerable to form conversion as compared to the other known anhydrous polymorphs of ritonavir. Process development details were previously published (*12*). Isolation of metastable forms is a routine aspect of polymorph screening, and though most often stable polymorphs are preferred for final drug products, metastable forms can be selected to improve dosing profiles or serve as enabling intermediates in manufacturing (*14,15*).

Results

Overview of Experiment

Figure 1 shows an exploded rendering and photo of the crystallization hardware contained within the spacecraft. The hardware features three stainless steel sample vials sealed with a stainless-steel screw-on cap. A PTFE sphere is seated between the cap and the ritonavir Form II powder to enable sealing of the powder under compression. The hardware is controlled with a printed circuit board (PCB) that enables the application of pre-programmed thermal profiles, established from ground-based studies on ritonavir's metastable Form III *(12)*. Temperature control is achieved through the use of film heaters and a Peltier device in thermal contact with the flight vials via an aluminum heat spreader.

Sample loading took place on October 21st, 2022. Flight vials were loaded with ~150 mg of ritonavir Form II. In addition to the three vials that underwent crystallization, four ritonavir control samples were placed in the capsule, thermally isolated from the crystallization hardware to ensure that no thermal profile would be applied to the controls. The purpose of these vials was to determine if any environmental factors experienced throughout the capsule's lifetime influence the final form of ritonavir. Examples of factors that could induce form conversion are vibration and shock events on ascent, radiation

from the orbital environment, shock events during reentry, and unwanted temperature increases throughout the process of re-entering the atmosphere and returning to Earth (*16,17*). Control Vial 1 contains amorphous ritonavir, Control Vial 2 contains Form I ritonavir, Control Vial 3 contains Form II ritonavir, and Control Vial 4 contains Form III ritonavir. The order of ritonavir's form stability is amorphous < Form III < Form I < Form II *(12,13)*.

In-orbit crystallization is performed inside a compact, unmanned capsule with Earth reentry capabilities. The reentry capsule and on-board crystallization hardware were developed by Varda Space Industries. Power, communication, and propulsion are provided by a Pioneer satellite bus (Rocket Lab, Inc.). The spacecraft was brought to orbit on a SpaceX Falcon 9 rocket on Transporter 8 launched June 12th, 2023. In-orbit crystallization experiments initiated on June 29th, 2023. The melt temperature was held for 36 minutes at 131 °C +/- 2 °C. The quench from the melt temperature to the growth temperature occurred at a rate of -50.9 °C/min where it reached a temperature of 77.3 °C before stabilizing. The growth phase temperature was set at 80 °C +/- 4.2 °C for 23.97 hours before cooling to 15 °C at a rate of -3.8 °C/min. A duplicate hardware set was operated back on Earth and used to confirm successful crystallization of Form III in a thermal vacuum chamber at a pressure of 0.001 Torr. Figure 2 shows the thermal profile of the terrestrial test compared to the thermal profile applied in microgravity.

After in-space crystallization, the capsule remained in orbit for approximately 8 months before safely landing at the Utah Test and Training Range on February 21st, 2024. During reentry the test vial temperature did not exceed 23 °C as shown in Figure 3.

Ritonavir Analysis

Upon removal from the capsule in Utah, the crystallized and control samples were sent in a temperature-controlled environment to the Improved Pharma facility in West Lafayette, IN to analyze the material in each vial. Figure 4 shows the X-ray powder diffraction (XRPD) data and Raman spectra of each of the flight vials compared to a reference of Form III. The analysis of all samples crystallized in microgravity indicates all samples consistent are crystalline Form III. Some amorphous background is detectable in the diffraction pattern of the flight vials. We determined that this amorphous background is likely introduced in the process of sample retrieval from the vials and sample preparation for XRPD as opposed to being introduced via factors from orbit or reentry. We were able to do so by isolating crystalline material above the PTFE ball which was removable while remaining intact. XRPD data of this confirmation is shown in the SI. Furthermore, evidence of amorphous material is not detected in the differential scanning calorimetry (DSC) thermogram indicating that the samples are predominantly crystalline Form III.

Figure 5 shows the XRPD diffractograms, Raman spectra, and DSC thermograms of the control vials that did not undergo crystallization in microgravity. All control samples, regardless of relative physical stability, were found to be of the same crystal form as packed without detectable amorphous background. This indicates that neither in-orbit radiation nor conditions upon reentry cause polymorph conversion of ritonavir or crystallization of the amorphous ritonavir. Table 1 summarizes the result of all vials in the W-1 capsule.

Discussion

Our presented results demonstrate the feasibility of processing pharmaceuticals in microgravity. Autonomous operation and reentry expand access to in-orbit processing of pharmaceuticals. The presented work demonstrates excellent thermal control both in-orbit and throughout recovery. For the thermal profile investigated, the polymorphic outcome for ritonavir crystallized from its melt is unchanged when compared to results on Earth. This result is due to the underlying crystallization mechanisms as well as the selection of a process that strongly favors formation of Form III (*12,18,19*). Future work will examine polymorphic outcomes in microgravity by not only examining additional molecules, but also by expanding the range of thermal profiles examined, including probing behavior at the interface between known or anticipated polymorphic outcomes. The results highlight the importance of careful considerations of crystallization kinetics, thermophysical properties of crystals and their melts, including density, viscosity, and diffusion coefficients alongside ground-based studies to help inform process sensitivity to gravitational forces (*20-22*). By demonstrating stability, this work enables a path towards in-space processing of pharmaceuticals that not only enables the development of novel drug products for use on Earth, but also contributes to the feasibility of long-duration human exploration initiatives.

Materials and Methods

Preparation of Ritonavir

Form II ritonavir was sourced from USP lot M-RIT/0804007. In the preparation of Form I, 206.3 mg of Form II Ritonavir was dissolved in approximately 6 mL or more of ethyl acetate (EtOAc) with the application of heat, approximately 70 °C. The solution was then allowed to cool to room temperature and left to stand overnight without any observable change. Subsequently, a rapid evaporation process was employed to reduce the volume by approximately half. To this concentrated solution, cold hexane (approximately 14 mL) was added slowly with continuous stirring, resulting in the immediate formation of a white precipitate which then transitioned into a sticky mass. The mixture was then vigorously vortexed, slightly warmed, and stirring was maintained at room temperature. Afterward, the mixture was placed in the freezer overnight. The resulting precipitant was recovered with filtration through a Swinnex filter assembly equipped with a nylon membrane of 25 mm diameter and 0.2 µm pore size.

In the preparation of Form III, 651.4 mg of Form II Ritonavir was evenly spread on a glass microscope slide and compressed to an approximate thickness of 1 mm. The slide was then placed in an oven set at roughly 130 °C, where the solid melted completely within about 25 minutes. After melting, the slide was transferred to an oven maintained at 80 °C and left there for approximately 24 hours. Upon removal, the sample was cooled to room temperature, and the presence of some crystals within the glass matrix was confirmed under a microscope. The sample was then returned to the 80 °C oven overnight, but no further changes were observed microscopically. Subsequently, the sample was placed back in the 130 °C oven, where it melted in roughly one minute. The oven temperature was then gradually reduced to approximately 83 °C, and the sample was left overnight. The following day, the white to light tan solids were removed from the oven and cooled to room temperature. The sample appeared fully crystalline under microscopic examination. The final step involved removing the crystalline material from the slide and gently crushing it into a fine powder.

In the preparation of the amorphous Ritonavir, 904.8 mg of Form II Ritonavir was placed on a glass microscope slide and compressed to approximately 1 mm thickness. The slide was then placed in an oven preheated to approximately 130 °C, where the solid melted completely within approximately 10 minutes. Following this, the molten sample was rapidly quenched on a cold aluminum block taken from the freezer. The sample was then carefully removed from the slide.

Each sample, weighing 150 ± 1 mg, was carefully transferred into vials within a glove bag purged with inert, dry nitrogen gas to ensure an oxygen- and moisture-free environment.

XRPD

XRPD patterns were collected on a PANalytical Empyrean diffractometer using a Cu Kα incident beam of radiation generated at 45 kV / 40 mA. A silicon standard was analyzed to verify the observed position of the Si <111> peak is consistent with the NIST-certified position. Powder samples were sandwiched between 3-µm-thick Etnom films and analyzed in transmission geometry. The X-ray source was configured with Soller slits of 0.02 radians, a fixed anti-scatter slit of 1/2°, a mask of 20 mm, and a fixed divergence slit of 1/2°. The diffracted beam passed through a 3.0 mm anti-scatter extension and Large Soller slits of 0.02 radians to the detector. A beam-stop was used to minimize the background generated by air. Diffraction patterns were collected with Data Collector software using a PIXcel3D-Medipix3 detector located 240 mm from the specimen. The data was acquired using a single scan from 2-50° 2θ with the sample spinning at a revolution time of 2 seconds.

Raman Spectroscopy

A HORIBA Scientific XploRA Series Confocal Raman Microscope (Piscataway, NJ) was used to collect Raman spectra using the following parameters: 785 nm laser at 100% power, 1200 g/mm grating, 300 micrometer confocal hole, 100 micrometer slit entrance to the spectrograph, 1 second spectra acquisition with 30 accumulations. The Raman signal is detected using a Syncerity Model 356399, thermoelectrically cooled CCD detector. Spectra were acquired over the range -125 to 1800 cm^{-1}. An Olympus Series BX51TRF polarized light microscope (Olympus America Inc., Melville, NY) provided the base optical platform. An Olympus MPlan N Series 20X, 0.40 NA microscope objective was used to focus the laser light onto the sample and to collect the Raman signal. The microscope was equipped with a Marzhauser Wetzlar computer-controlled mapping stage to translate the sample for focus and data acquisition. Digital images were acquired using a Lumenera Series Infinity 3-1C (Teledyne Lumenera, Ottawa, Ontario, Canada) camera using Infinity software version 6.5.6 and Infinity Analyze software version 7.0.2.930 (Build data 1-May-2020). System calibration was performed prior to analysis using a silicon disc to monitor peak position at 520.7 cm^{-1}.

The sample was prepared for analysis by placing a small amount of material onto a gold-coated microscope slide using a tungsten needle and dispersed to a thin layer. The small sample was illuminated with white light using 200X magnification for specific sample area analysis.

DSC

DSC was performed using a TA Instruments model Q10 differential scanning calorimeter. The instrument was calibrated using indium. The sample was placed into a standard aluminum DSC pan, covered with a lid that was manually pierced with a pin, and the weight was accurately recorded. The pan lid was crimped prior to sample analysis. An aluminum pan configured as the sample pan was placed on the reference side of the cell. The sample was analyzed in a single run from 20 to 200 °C at a heating rate of 10 °C/min under a purge of nitrogen (50 cc/min).

References

1. Y. Zhang, J. Cheng, Y. Glick, G. Samburski, J. Chen, C. Yang, Antisolvent crystallization of L-histidine in micro-channel reactor under microgravity *Microgravity Science and Technology* **32**, 27-33 (2020).
2. S. Amselem Remote controlled autonomous microgravity lab platforms for drug research in space *Pharmaceutical Research* **36**, 183 (2019).
3. M. A. Giulianotti and L. A. Low, Pharmaceutical research enabled through microgravity: Perspectives on the use of the international space station U.S. national laboratory *Pharmaceutical Research* **37**, 1 (2020).
4. P. Reichert, W. Prosise, T. O. Fischmann, G. Scapin, C. Narasimhan, A. Spinale, R. Polniak, X. Yang, E. Walsh, D. Patel, W. Benjamin, J. Welch, D. Simmons, C. Strickland, Pembrolizumab microgravity crystallization experimentation *npj Microgravity* **5**, A28 (2019).
5. S. R. Byrn, R. R. Pfeiffer, J. G. Stowell *Solid-state chemistry of drugs* (SSCI, Inc., 1999).
6. J. Bauer, S. Spanton, R. Henry, J. Quick, W. Dziki, W. Porter, J. Morris, Ritonavir: an extraordinary example of conformational polymorphism *Pharmaceutical Research* **18**, 859-866 (2001).
7. P. M. Williams, T. Shivakumar, V. Anyanwu, “Space Medicine and Countermeasures” in *In-Space Manufacturing and Resources* (Wiley Online Books, 2022).
8. J. F. Reichard, S. E. Phelps, K. R. Lenhardt, M. Young, B. D. Easter, The effect of long-term spaceflight on drug potency and the risk of medication failure *npj Microgravity* **9**, A35 (2023).
9. M. Gresko, Panel calls for giant boost to space station research *Science* **381**, 1144-1145 (2023).
10. J. Foust, NASA hits limits of space station utilization *Space News* (January 31, 2023).
11. J. Foust, SpaceX revamps smallsat rideshare program *Space News* (August 29, 2019).
12. S. D. Parent, P. A Smith, D. K. Purcell, D. T. Smith, S. J. Bogdanowich-Knipp, A. S. Bhavsar, L. R. Chan, J. M. Croom, H. C. Bauser, A. McCalip, S. R. Byrn, A. Radocea, Ritonavir form III: A coincidental concurrent discovery *Crystal Growth & Design* **23**, 320-325 (2022).
13. X. Yao, R. F. Henry, G. G. Z. Zhang, Ritonavir Form III: A new polymorph after 24 years *Journal of Pharmaceutical Sciences* **112**, 237-242 (2022).

14. R. Censi and P. D Martino, Polymorph impact on the bioavailability and stability of poorly soluble drugs *Molecules* **10,** 18759-18776 (2015).
15. A. Y. Sheikh, A. Mattei, R. M. Bhardwaj, R. S. Hong, N. A. Abraham, G. Schneider-Rauber, K. M. Engstrom, M. Diwan, R. F. Henry, Y. Gao, V. Juarez, E. Jordan, D. A. DeGoey, C. H. Hutchins, Implications of the conformationally flexible, macrocyclic structure of the first-generation, direct-acting anti-viral paritaprevir on its solid form complexity and chameleonic behavior *Journal of the American Chemical Society* **143**, 17479-17491 (2021).
16. "Rideshare Payload User's Guide (SpaceX, 2021).
17. R. G. Finke, Calculation of reentry-vehicle temperature history *Institute for Defense Analysis* IDA Paper P-2395 (1990).
18. M Mohr and H. Fecht, Investigating thermophysical properties under microgravity: A review *Advanced Engineering Materials* **23**, 2001223 (2021).
19. J. A. Baird, B. Van Eerdenbrugh, L. S. Taylor, A classification system to assess the crystallization tendency of organic molecules from undercooled melts *Journal of Pharmaceutical Science* **99,** 3787-3806 (2010).
20. P. W. G. Poodt, P. C. M. Christianen, W. J. P. van Enckevort, J. C. Maan, E. Vlieg. The critical Rayleigh number in low gravity crystal growth from solution *Crystal Growth and Design* **,** 2194-2199 (2008).
21. E. H. Snell and J. R. Helliwell, Macromolecular crystallization in microgravity *Reports on Progress in Physics* **68**, 799 (2005)
22. K. Pal and A. Radocea, Gravity as a knob for tuning particle size distributions of small molecules *Crystal Growth and Design* (2024).

Acknowledgments

The authors acknowledge the mission operations team at Varda Space Industries and Rocket Lab, Inc. for their work in maintaining the capsule throughout its life cycle. The authors acknowledge Brandon Amat, Tracy Vu, and Kris Stone for their recovery of the capsule and safe retrieval of the experimental vials. The authors acknowledge Aakash Patel for integration and testing support. The authors acknowledge Sarah Parent for her photography of the hardware.

Author contributions:

Conceptualization: AR, JMC, SRB. HCB
Hardware Development: LRC, ASB, KHC, AM, JMC
Process Development: HCB, SRP, PAS, BAC, ASB, JMC, AR
Analysis: PAS, SRP, HCB, RAA, DKP, SJB, DTS
Writing—original draft: HCB
Writing—review & editing: HCB, AR, PAS.

Competing interests: The authors declare the following competing financial interest(s): Varda Space Industries participated in the experimental design, research, data interpretation and analysis, writing, reviewing, and approval of the publication. H.C. Bauser, A.S. Bhavsar, A. McCalip, L.R. Chan, K. H Condon, J.M. Croom, and A.

Radocea are employees of Varda Space Industries and may own Varda Space Industries stock.

Data and materials availability:

All data are available in the main text or the supplementary materials.

Figures and Tables

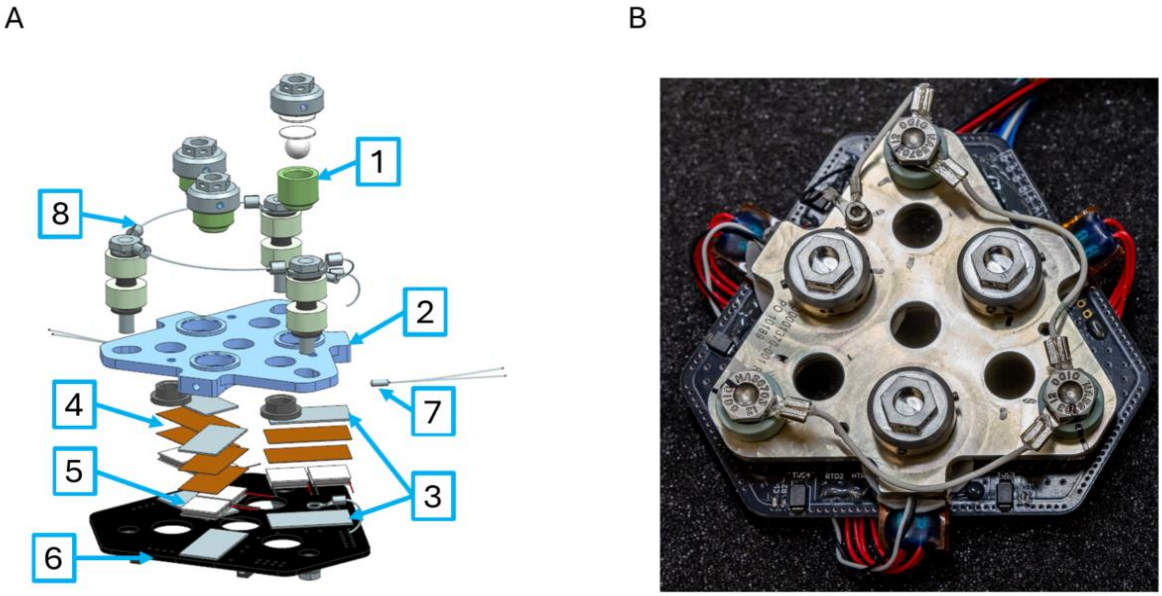

Fig. 1. Overview of the in-orbit crystallization hardware. (A) Exploded view of the Varda PCB Stack and API vials. The components are as follows. 1) (3x) 316 Stainless Steel vials each holding ~150 mg of API, sealed with a PTFE ball and spacers. 2) 6061 Aluminum plate heat spreader holding the vials and the resistance temperature detectors (RTDs). 3) Thermal interface material 4) (6x) Kapton film heaters each with a total power of 23 watts 5) (6x) Peltier devices used in both forward bias for cooling and reverse bias for additional heater power 6) PCB 7) (2x) RTDs in heat spreader and 1x RTD on the ballast side of the PCB 8) grounding wires. **(B)** Picture of the fully assembled Varda PCB Stack.

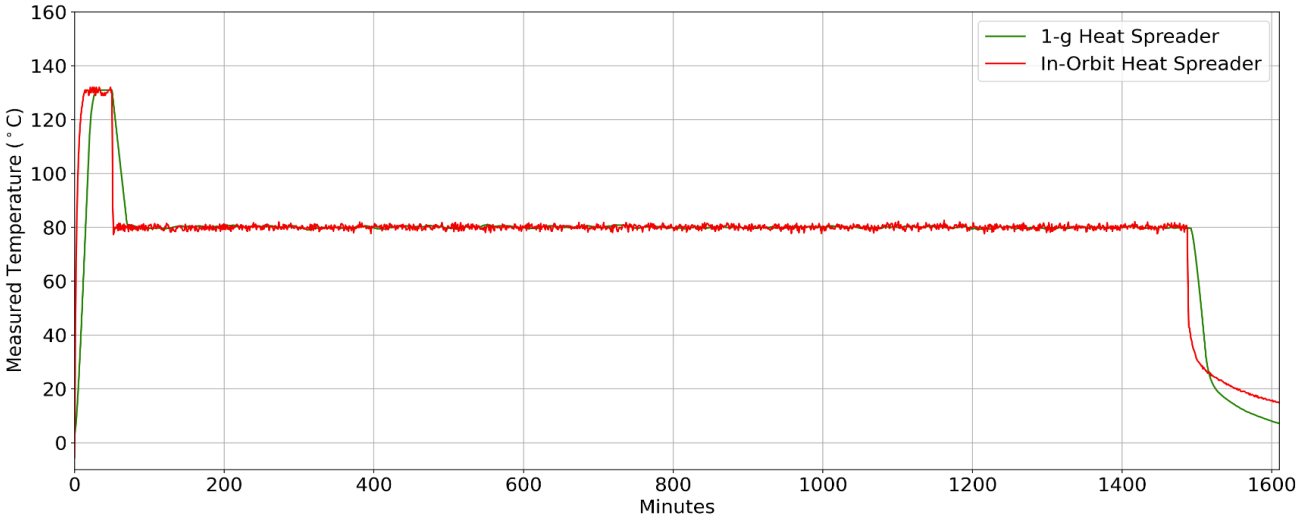

Fig 2. Temperature Profile in 1-g and In-Orbit. Comparison of the heat spreader temperature during the 1-g crystallization of ritonavir and the heat spreader temperature during the in-orbit crystallization of ritonavir.

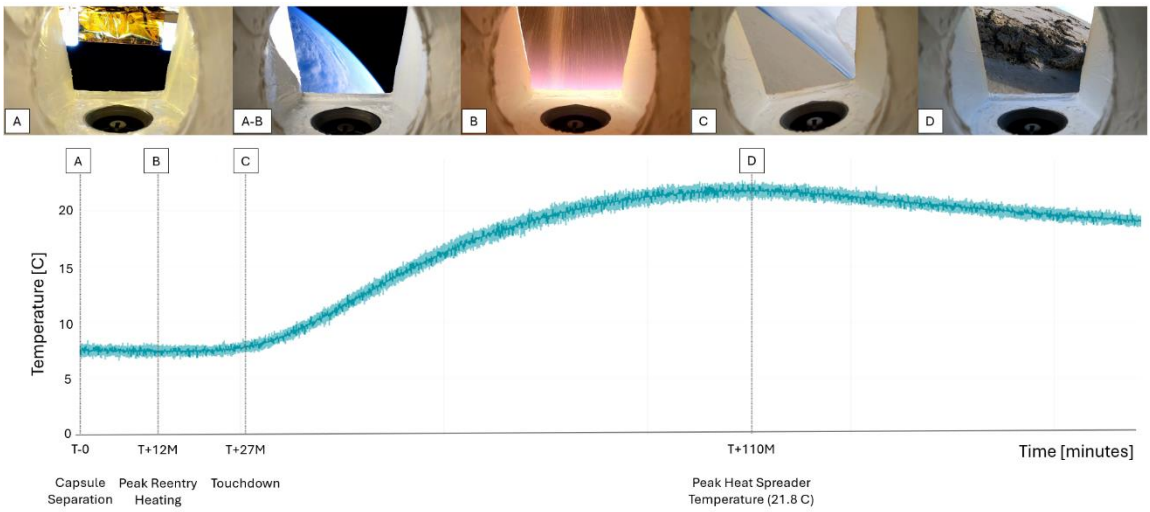

Fig 3. Timeline of Heat Spreader Temperature Throughout Reentry with Corresponding Images from Capsule. (A) Image and corresponding heat spreader temperature upon capsule separation from the Pioneer satellite. **(A-B)** Image shows the capsule above Earth independent of the satellite. **(B)** Image and corresponding heat spreader temperature at the maximum capsule external temperature during reentry. **(C)** Image and corresponding heat spreader temperature upon capsule touchdown in Utah. **(D)**

Image and corresponding heat spreader temperature at maximum temperature experienced while awaiting recovery.

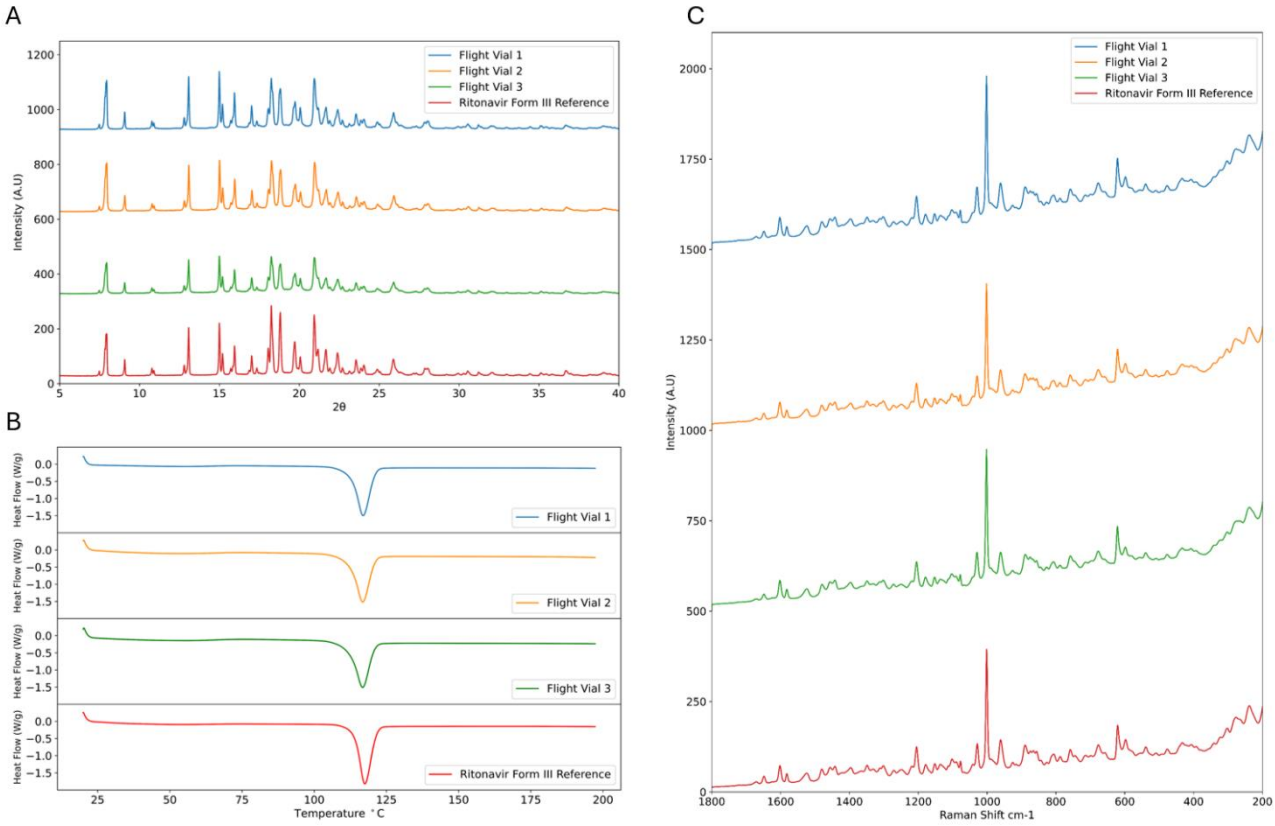

Fig 4. Analysis of Samples Crystallized in Microgravity. (A) Diffractograms of material extracted from each of the three vials that underwent crystallization in-orbit. All three vials match the Form III reference material. **(B)** Thermograms of material extracted from each of the three vials that underwent crystallization in-orbit. All three vials match the endotherm of Form III. The melt temperatures are 116.94 °C, 116.77 °C, 116.73 °C, respectively and the heat capacities are 50.54 J/g, 51.78 J/g, and 51.11 J/g, respectively **(C)** Raman spectra of material extracted from each of the three vials that underwent crystallization in orbit. The presented spectra are averages of the spectra of 10 samples from each of the vials to ensure adequate representation across the crystalline material.

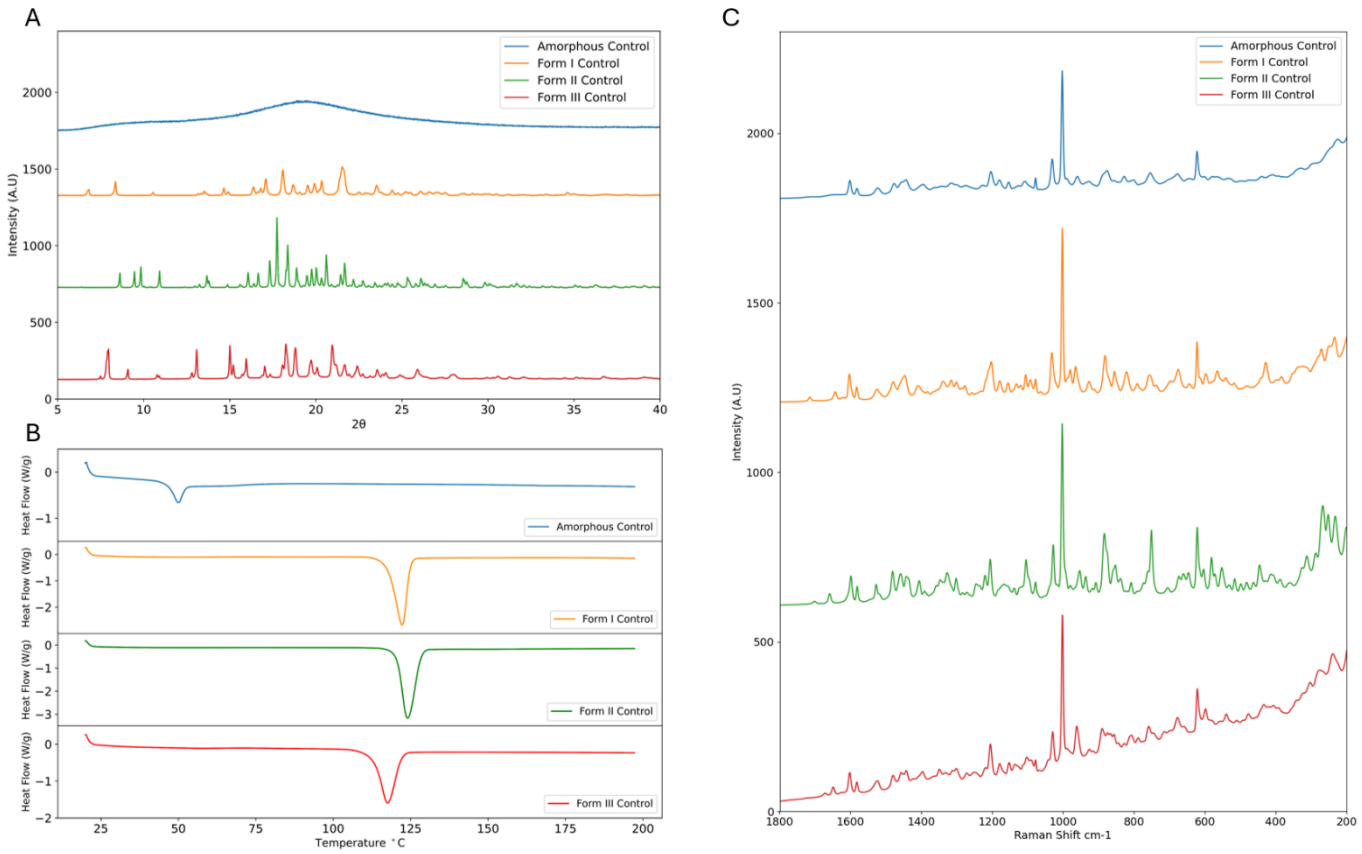

Fig 5. Analysis of In-Orbit Control Samples. (A) Diffractograms of material extracted from the control vials. All diffraction patterns match that of their initially packed form **(B)** Thermograms of material extracted from each of the control vials. All endotherms match that of their form as packed. The melting temperatures are 50.0 °C, 122.25 °C, 124.00 °C, and 117.52 °C, respectively. The heat capacity of Form I is 76.46 J/g, the heat capacity of Form II is 94.23 J/g, and the heat capacity of Form III is 53.13 J/g. **(C)** Raman spectra of material extracted from the control vials. All spectra match that of their initially packed form. The presented spectra are each an average of the spectra of 10 samples from each of the vials to ensure adequate representation across the crystalline material.

411 **Table 1. Summary of Flight Sample Crystallinity**

Sample ID	Starting Material	In-Orbit Crystallization	Post Reentry Material
Flight Vial 1	Ritonavir Form II	Yes	Ritonavir Form III
Flight Vial 2	Ritonavir Form II	Yes	Ritonavir Form III
Flight Vial 3	Ritonavir Form II	Yes	Ritonavir Form III
Control Vial 1	Amorphous Ritonavir	No	Amorphous Ritonavir
Control Vial 2	Ritonavir Form I	No	Ritonavir Form I
Control Vial 3	Ritonavir Form II	No	Ritonavir Form II
Control Vial 4	Ritonavir Form III	No	Ritonavir Form III

412